Published in final edited form as:
J Nanotechnol Eng Med. 2010 August 1; 1(3): . doi:10.1115/1.4001934.

A Distinct Catabolic to Anabolic Threshold Due to Single-Cell Static Nanomechanical Stimulation in a Cartilage Biokinetics Model

Asit K. Saha and
Center for Allaying Health Disparities through Research and Education (CADRE), Department of Mathematics and Computer Science, Central State University, Wilberforce, OH 45384

Sean S. Kohles[1]
Reparative Bioengineering Laboratory, Department of Mechanical and Materials Engineering, Portland State University, Portland, OR 97201; Department of Surgery, Oregon Health and Science University, Portland, OR 97201

Asit K. Saha: asaha@centralstate.edu; Sean S. Kohles: kohles@cecs.pdx.edu

Abstract

Understanding physicochemical interactions during biokinetic regulation will be critical for the creation of relevant nanotechnology supporting cellular and molecular engineering. The impact of nanoscale influences in medicine and biology can be explored in detail through mathematical models as an in silico testbed. In a recent single-cell biomechanical analysis, the cytoskeletal strain response due to fluid-induced stresses was characterized (Wilson, Z. D., and Kohles, S. S., 2010, "Two-Dimensional Modeling of Nanomechanical Strains in Healthy and Diseased Single-Cells During Microfluidic Stress Applications," J. Nanotech. Eng. Med., **1**(2), p. 021005). Results described a microfluidic environment having controlled nanometer and piconewton resolution for explorations of multiscale mechanobiology. In the present study, we constructed a mathematical model exploring the nanoscale biomolecular response to that controlled microenvironment. We introduce mechanical stimuli and scaling factor terms as specific input values for regulating a cartilage molecule synthesis. Iterative model results for this initial multiscale static load application have identified a transition threshold load level from which the mechanical input causes a shift from a catabolic state to an anabolic state. Modeled molecule homeostatic levels appear to be dependent upon the mechanical stimulus as reflected experimentally. This work provides a specific mathematical framework from which to explore biokinetic regulation. Further incorporation of nanomechanical stresses and strains into biokinetic models will ultimately lead to refined mechanotransduction relationships at the cellular and molecular levels.

1 Introduction

Understanding the structure, function, and regulation of biological systems in real time at the nanoscale level is a challenging task. Nanobioscience is a newly emerging field where investigators describe the smallest molecular structures and their dynamics in the realm of space and time. Clarifying the functions of cells and biomolecules within the extracellular space will provide the basis for the development of nanoscale devices mimicking and/or influencing biological processes. Knowledge about the topology of the cells, biomolecules, and their mutual interactions at the nanoscale will provide insight regarding fundamental

[1]Corresponding author.

biological functions, which are absolutely necessary in the development of new tissues and/or controlling tissue remodeling.

At the nanoscale level, physiologic regulation of cartilage biomolecules is maintained by chondrocytes although they are sparsely distributed within the tissue and are low in number [1–3]. Cell-cell and cell-extracellular matrix (ECM) interactions and subsequent communication are very important in tissue development, remodeling, and homeostasis. In normal or pathological situations, cartilage ECM homeostasis is dependent upon nanoscale anabolic and catabolic pathways controlled by the chondrocytes [4,5]. Ironically, chondrocytes have dual roles; they produce both the structural macromolecules in tissue formation, such as collagen and proteoglycans, as well as a variety of metalloproteinases, such as collagenase, gelatinase, stromelysin, and aggrecanase, which are responsible for tissue turnover (Fig. 1). Structural protein molecules consist of type II collagen and elastin. Specialized protein molecules consist of fibrillin, fibronectin, laminin, and, lastly, proteoglycans, which are core protein molecules to which long chains of repeating disaccharide units known as glycosaminoglycans (GAG) are attached. The mechanical behavior of cartilage is strongly influenced by constituent content and the electrostatic forces between matrix charge groups [6].

During healthy balanced regulation, the growth factors such as transforming growth factor-β (TGF-β), insulin-like growth factor-1 (IGF-1), and osteogenic protein-1 (OP-1) stimulate the chondrocytes to synthesize the structural macromolecules, such as collagen and proteoglycan (anabolic modulation), while cytokines interleukin-1 (IL-1), interleukin-6 (IL-6), and tumor necrosis factor-α (TNF-α) stimulate chondrocyte secretion of proteinases, causing ECM degradation (catabolic modulation). It is now obvious that growth, maintenance, and degradation of cartilage ECM are dependent on a balance between molecular (nanoscale) anabolic and catabolic activities. In the case of cartilage matrix growth and repair/remodel, anabolic processes exceed the catabolic activities. Alternatively, catabolic processes exceed anabolic activities when disease and degeneration are at hand. These relationships have been observed in controlled osteoarthritic culture models where experimental results show that the combination of anabolic growth factors and protective catabolic blockers may be a means for partial restoration of the cartilage matrix [7]. Therefore, any alterations in the molecular regulatory balance between anabolic and catabolic signaling can lead to multiscale pathology (tissue, joint, etc.) including osteoarthritis [8].

The question arises as to whether growth factors and cytokines are solely responsible for maintaining the balance between the anabolic and catabolic regulatory mechanisms, or is some other mechanism involved in this complex process. It has been observed that physical movements and applied mechanical forces maintain healthy cartilage tissue [9,10]. The structural organizations of collagen and proteoglycan in the articular cartilage vary along the depth of the tissue influencing the load-bearing capacity of the tissue. A reduction in the thickness of the cartilage tissue has been observed during an absence of mechanical loading [10]. In the articular cartilage, the concentration of lubricating molecules (such as lubricin) is high around the surface, whereas higher concentrations of aggrecans are found in deeper zones [11,12]. Applied mechanical compression results in a deformity of the cartilage structural molecules while subsequent unloading causes the influx of nutrients from the surrounding synovial fluid into the tissue [13–15]. However, the mechanical influence on the balanced regulatory molecular network of anabolic and catabolic pathways has not been fully described, including the maintenance of ECM homeostasis at the nanoscale level [8].

It has been observed in both in vivo and in vitro environments that injurious loading caused by high mechanical compression of cartilage results in cell apoptosis [16,17] as well as

increased degradation and decreased synthesis of matrix structural molecules [18–21]. A similar scenario was observed in tissue engineered constructs where dynamic mechanical stresses influenced the biosynthesis of matrix molecules and accumulation while concurrently reducing the intensity of the catabolic process [22–27]. Alternatively, static loads inhibited the synthesis of matrix biomolecules [22,28].

In our previous predictions of articular cartilage matrix synthesis, an approach was based on systems biology. Our results clearly indicate that anabolic actions of different growth factors are essentially dose and time dependent [29,30]. These works have culminated in characterizing molecular regulatory mechanisms influencing both anabolic and catabolic processes, which maintain matrix homeostasis [31]. With advances in single-cell biomechanics and nanomechanical modeling, the dynamics of anabolic and catabolic pathways can now be extended to include mechanical stimuli, be it static or dynamic [32,33]. The objective of this study is to link the complex dynamics of the molecular anabolic and catabolic pathways with nanomechanical stimuli at the single-cell level. This mathematical modeling approach comes from a systems point of view to help explain the multiscale feedback effects of the anabolic and catabolic actions within an engineered cartilage platform.

2 Materials and Methods

2.1 Mathematical Model

Based on previous studies, it can be concluded that there exists a dynamic relationship between anabolic and catabolic activities, which regulates matrix homeostasis. The important anabolic proteins are various growth factors, and the important catabolic protein includes cytokines. During healthy balanced regulation, growth factors such as TGF-β, IGF-1, and OP-1 stimulate the chondrocytes to synthesize the structural macromolecules, while cytokines such as IL-1, IL-6, and TNF-α stimulate chondrocyte secretion of proteinases, causing ECM degradation.

For the mathematical model, let [C], [G], and [E] represent the nanoscale concentration of biomolecules representing cytokines, growth factors, and ECM, at any particular time, t. According to the schematic relationships (Fig. 1), the mathematical model is defined as follows:

$$\begin{aligned}\frac{d[C]}{dt}&=\eta_1[C]\{\Re_2-[G]\}-\mu_1[C]\\ \frac{d[G]}{dt}&=\eta_2[G]\{[C]-\Re_1\}-\mu_2[G]\\ \frac{d[E]}{dt}&=\frac{v[G]}{K+[C]}-\sigma[E]\end{aligned} \tag{1}$$

where η_i denotes the overall growth rates, μ_i denotes the overall degradation rates, v is the growth rate for ECM production, σ is the natural degradation rate of ECM, K is the saturation parameter, $\Re_i$ is the pivotal concentration for subscripts equaling (i=1, cytokines, and 2, growth factors).

The dimensionless form of the modeled system can be written as

$$\begin{aligned}\frac{d}{dT}\begin{pmatrix}C\\G\end{pmatrix}&=\begin{pmatrix}f_1(C,G,\alpha_1,\beta_1,\Omega_2)\\f_2(C,G,\alpha_2,\beta_2,\Omega_1)\end{pmatrix}\\ \frac{d}{dT}E&=f_3(C,G,E,\lambda,\delta)\end{aligned} \tag{2}$$

where

$$\begin{array}{cccc} C=K^{-1}[C], & G=K^{-1}[G], & E=K[E], & T=K^{2}[t] \\ \alpha_1=K^{-1}\eta_1, & \alpha_2=K^{-1}\eta_2, & \beta_1=K^{-2}\mu_1, & \beta_2=K^{-2}\mu_2 \\ \lambda=K^{-1}v, & \delta=K^{-2}\sigma, & \Omega_1=K^{-1}\Re_1, & \Omega_2=K^{-1}\Re_2 \end{array} \tag{3}$$

and

$$\begin{array}{c} f_1(C,G,\alpha_1,\beta_1,\Omega_2)=\alpha_1 C(\Omega_2-G)-\beta_1 C \\ f_2(C,G,\alpha_2,\beta_2,\Omega_1)=\alpha_2 G(C-\Omega_1)-\beta_2 C \\ f_3(C,G,E,\lambda,\delta)=\frac{\lambda G}{1+C}-\delta E \end{array} \tag{4}$$

Here, the first equation in system (2) describes both the anabolic and catabolic actions of cytokines and growth factors, whereas the second equation demonstrates the synthesis dynamics of the ECM.

The kinetic conditions are now divided into two environments, with and without applied mechanical stresses. In the mechanical stress environment such as experienced in vivo, the system experiences a constant mechanical stimulus. In this mechanical loading system, Eq. (2) can be written as

$$\begin{array}{c} \frac{d}{dT}\begin{pmatrix} C \\ G \end{pmatrix}=\begin{pmatrix} f_1(C,G,\alpha_1,\beta_1,\Omega_2) \\ f_2(C,G,\alpha_2,\beta_2,\Omega_1) \end{pmatrix}+\begin{pmatrix} \rho_1 & 0 \\ 0 & \rho_2 \end{pmatrix}\begin{pmatrix} \xi_1(T) \\ \xi_2(T) \end{pmatrix} \\ \frac{d}{dT}E=f_3(C,G,E,\lambda,\delta) \end{array} \tag{5}$$

where $\begin{pmatrix} \xi_1(T) \\ \xi_2(T) \end{pmatrix}$ represents the applied mechanical stimuli and $\begin{pmatrix} \rho_1 & 0 \\ 0 & \rho_2 \end{pmatrix}$ denotes scaling factor coefficients associated with this influence on cytokine (C) and growth factor (G) dynamics.

2.2 Steady State Condition (Homeostasis)

In a mechanically protected system where a physical “shielding” and no mechanical loading occurs, the nontrivial steady state and/or equilibrium levels of the constituents (C_{ss},G_{ss},E_{ss}) can be obtained from the following set of equations [31]:

$$\begin{pmatrix} C_{ss} \\ G_{ss} \\ E_{ss} \end{pmatrix}=\begin{pmatrix} \Delta_1 \\ \Delta_2 \\ \frac{\lambda\Delta_2}{\delta(1+\Delta_1)} \end{pmatrix} \tag{6}$$

where $\Delta_1 = \Omega_1 + \beta_2/\alpha_2$ and $\Delta_2 = \Omega_2 - \beta_1/\alpha_1$.

The two main biomolecular constituents of ECM considered here are type II collage, the structural proteins, and proteoglycans. Proteoglycans are the core proteins to which are attached long chains of repeating disaccharide units known as GAG. As shown previously for steady state ECM,

$$E_{ss} \approx \text{Collagen}_{ss} + \text{GAG}_{ss} = \frac{\lambda\left(\Omega_2 - \frac{\beta_1}{\alpha_1}\right)}{\delta\left(1 + \Omega_1 + \frac{\beta_2}{\alpha_2}\right)} \tag{7}$$

If we assume that the synthesis of collagen and GAG molecules are independent, then we can separate the ECM components and rewrite the system in a fashion similar to Eq. (2), such as

$$\frac{d}{dT}\begin{pmatrix} \text{GAG} \\ \text{Collagen} \end{pmatrix} = \begin{pmatrix} \frac{\lambda_1 G}{1+C} - \delta_1(\text{GAG}) \\ \frac{\lambda_2 G}{1+C} - \delta_2(\text{Collagen}) \end{pmatrix} \tag{8}$$

The steady state conditions of the GAG and collagen components can then be defined as

$$\begin{pmatrix} \text{GAG}_{ss} \\ \text{Collagen}_{ss} \end{pmatrix} = \begin{pmatrix} \frac{\lambda_1\left(\Omega_2 - \frac{\beta_1}{\alpha_1}\right)}{\sum} \\ \frac{\lambda_2\left(\Omega_2 - \frac{\beta_1}{\alpha_1}\right)}{\sum} \end{pmatrix} \tag{9}$$

where

$$\sum = \delta\left(1 + \Omega_1 + \frac{\beta_2}{\alpha_2}\right) > 0$$

A phase-space diagram of this dynamic system indicates accumulation-dependent zones delineated by an abscissa representing cytokine levels and an ordinate indicating growth factor status, intersecting at a homeostatic origin (C_{ss},G_{ss}) [31].

3 Biomolecular Simulation

Normalized parameter estimation associated with anabolic/catabolic activity was made through a mathematical association between growth factor/cytokine abundance in the development of sweat glands in human fetal skin [34,31]. These input parameters provided the synergistic effects of cytokines and growth factors over a time frame typical of recent engineered cartilage culture scenarios [32].

The overall parameter estimations include biokinetic and biomechanical factors (Tables 1 and 2). The parameters characterizing ECM structural molecule and proteoglycan dynamics were determined previously through a deterministic approach where kinetic rate ratios of synthesis per decay contribute to steady state levels of ECM accumulation [30]. The parameters associated with mechanical stress and strain within isolated cartilage cells were also derived from previous analyses. These works determined the experimental and theoretical stresses applied to suspended cell-sized polystyrene microspheres within microfluidic environments designed for biological cell investigations. The stress analysis showed that fluid-induced stresses on suspended cells ranged from 0.02 Pa to 0.04 Pa during physically limited in vitro experiments [32]. However, the numerical strain analysis

indicated the required applied stresses nearing 10.0 Pa to elicit an appreciable strain response depending on the health (and stiffness) of the cell [33].

Iterative analyses of the described biokinetic models were run through 5000 normalized time steps using commercial software (MATHCAD 14.0, Parametric Technology Corp., Needham, MA). A range of nano- to mesomechanical stimuli identified in the previous single-cell studies was included in the time modeling iterations through the normalized parameters, ξ_i and ρ_i, introduced in Eq. (5). For this study, the load scaling factors were held constant at $\rho_1(T) = \rho_2(T) = 1$; however, this parameter can be further manipulated for enhanced resolution. Normalized load components were stepped through molecular-cellular (ξ_i=0.0 to 1.0) and cellular-tissue (ξ_i=1.0 to 100.0) scale ranges based on previous multiscale modeling [35]. Biokinetic thresholds were identified based on the transition from catabolic (ECM decrease) to anabolic (ECM increase) responses during the homeostatic “culture” time iterations.

4 Results

A mathematical framework has been presented, which characterizes nanoscale biokinetic mechanisms as stimulated within the micromechanical environment of a single cell. The overall impact of the mechanical stress has influenced the two fundamental regulatory processes, namely, anabolic and catabolic pathways, which lead to matrix homeostasis. The time-dependent GAG and collagen accumulation is shown in dimensionless form where the mechanical stress lies in the interval $0.0 \leq \xi(T) \leq 1.0$ with scaling factors $\rho_1 = \rho_2 = 1$ (Figs. 2–4). The imposed mechanical stress is considered here as a constant function over time; i.e., it is represented as a static mechanical stimulus. Three different experimental data sets have been considered [36–38].

Comparing the results with input data from previous work [36], the static mechanical stress in the range of $0.0 \leq \xi(T) \leq 1.0$ may have little influence on GAG accumulation toward matrix homeostasis (Figs. 2(a)–2(c)). However, the collagen accumulation attains peak values within a very short period of time when there is no mechanical stress. One can assume from a system dynamics point of view this peak value as a “pseudo-steady-state,” which is unstable. From the simulation, the system attained this pseudo-steady-state around the 2000th dimensionless time step. If there is no mechanical stress applied, the collagen accumulation eventually attains a permanent steady state at a much lower value, at least 50% less than its peak value, in a longer time frame (Fig. 2(a)). A threshold biokinetic response was observed in the model as the mechanical stress state was increased in scale (Figs. 2(b) and 2(c)), although GAG accumulation was minimally affected by the stimulation.

From an alternative data set [37], an intrinsic rate increase (growth rate minus decay rate) of GAG molecules was observed to be much higher than that of collagen. As a consequence, GAG accumulation was much higher than collagen accumulation (Figs. 3(a)–3(c)). However, it appears that collagen accumulation was less sensitive to lower levels of mechanical stimuli ($\xi \leq 0.02$) than GAG, requiring greater stimulation to reach homeostatis. In a third data set [38], the amount of accumulation between the GAG and collagen molecules also differed (Figs. 4(a)–4(c)). However, their kinetic sensitivity to mechanical stimulation appeared similar with a higher homeostatic threshold ($\xi \leq 1.0$).

The phase-space dynamics of the anabolic and catabolic pathways under an increasing influence of mechanical stimuli, $1.0 \leq \xi(T) \leq 100.0$, is demonstrated (Fig. 5). In a previous work [31], it was observed that the matrix molecules attain an apparent homeostasis within a very short period of time without any mechanical stimuli. The oscillatory dynamics between anabolic and catabolic interactions is shown. As the amplitude of oscillation becomes

damped over time, this apparent homeostasis no longer remains stable (Figs. 2(a), 3(a), and 4(a)). Low level static mechanical stimuli, $0.0 \leq \zeta(T) \leq 1.0$, makes the oscillatory network of anabolic and catabolic pathways further damped. As a consequence, the matrix molecules attain a much lower concentration at homeostasis. Results indicate the altered dynamics of anabolic and catabolic when the mechanical stimuli are increased beyond 1.0. Here, a higher mechanical stress threshold may dominate the anabolic pathway over catabolic actions (Fig. 5(c)), and higher transient values of matrix accumulation are expected.

5 Discussion

Results presented here offer a unique perspective toward understanding the influence of mechanical stimulation on biomolecule homeostasis. Scientists have conducted extensive research to understand this process of mechanotransduction, especially with regard to cartilage biology. Unfortunately, very little is known regarding how mechanical loading modulates the dynamics of the biochemical activity through changes in the cellular kinetics. Multiaxial applied stresses at the mesoscale (tissue) level result in complex changes at the nanoscale (molecular) level. These influences include ECM and cell deformation, changes in hydrostatic pressure gradients and fluid flow, changes in ion concentration and fixed charged density, etc. [39]. The mechanical stimuli may be of different types such as structural deformation of intracellular biomolecules or kinetic changes in the interactions of different extracellular biomolecules, all resulting in cell-mediated biosynthesis. Chondrocyte mechanoreceptors such as mechanosensitive ion channels [40] and integrins [41] are likely to be involved in recognition of these physiochemical changes. Most of the research has focused on signaling pathways that transduce mechanical stimuli in cartilage [16,42–57]. These studies generally indicate that multiple signaling pathways are covariate and interactive within the mechanotransduction process. Recent advancements in cartilage tissue engineering research also advocate that there are multiple pathways by which chondrocytes sense and respond to mechanical stimuli [58]. Mechanical stimuli at the nanoscale can influence cells in different ways, such as by epigenetic regulatory mechanism that controls genetic transcription and translation processes. The level of influence may, in turn, affect cell-mediated matrix assembly and degradation. The study presented here has taken a systems biology approach to examine the multiscale influences on the biokinetics of mechanotransduction.

Here, we investigated the impact of static mechanical stress on two fundamental pathways of matrix homeostasis, namely, anabolic and catabolic pathways. Our model simulations show that there is a distinct decrease in matrix molecule accumulation during homeostasis if the static mechanical loading stimulus is very low. Similar results obtained by experimentalists conclude that static compression significantly inhibits the synthesis of proteoglycans and other protein molecules [59,60].

Although limited to the static loading case, our simulation predicts that a sustainable harmonic balance between the two important pathways may be the key to obtain a stable matrix homeostasis. The static loading model attempts to attain the matrix homeostasis but with very low accumulation compared to the absence of mechanical loading. Higher order static and dynamic mechanical stimulation may drive the modeled system toward attaining homeostasis at a much higher level of accumulation. Ongoing efforts will build on the presented mathematical framework and explore the complexities of these unique system dynamics.

Acknowledgments

Support was provided by the National Institutes of Health as a Research Infrastructure for Minority Institutions (RIMI) Exploratory Program grant (Grant No. P20MD003350) established the CSU Center for Allaying Health Disparities through Research and Education (CADRE) and a PSU Academic Research Enhancement Award (Grant No. R15EB007077). Support was also provided by the Collins Medical Trust and a Portland State University Faculty Enhancement Grant.

References

1. Caplan AI. Cartilage. Sci Am 1984;251(4):84–94. [PubMed: 6435245]
2. Roughley PJ, Lee ER. Cartilage Proteoglycans: Structure and Potential Functions. Microsc Res Tech 1994;28:385–397. [PubMed: 7919526]
3. Buckwalter JA, Mankin HJ. Articular Cartilage, Tissue Design and Chondrocytes Matrix Interactions. Instr Course Lect 1997;47:477–486. [PubMed: 9571449]
4. Chambers MG, Bayliss MT, Mason RM. Chondrocyte Cytokine and Growth Factor Expression in Murine Osteoarthritis. Osteoarthritis Cartilage 1997;5:301–308. [PubMed: 9497937]
5. Moos V, Fickert S, Muller B, Weber U, Sleper J. Immunohistological Analysis of Cytokine Expression in Human Osteoarthritic and Healthy Cartilage. J Rheumatol 1999;26:870–879. [PubMed: 10229409]
6. Lee RC, Frank EH, Grodzinsky AJ, Roylance DK. Oscillatory Compressional Behavior of Articular Cartilage and Its Associated Electromechanical Properties. ASME J Biomech Eng 1981;103:280–292.
7. Haupt JL, Frisbie DD, McIlwraith CW, Robbins PD, Ghivizzini S, Evans CH, Nixon AJ. Dual Transduction of Insulin-Like Growth Factor-I and Interleukin-1 Receptor Antagonist Protein Controls Cartilage Degradation in an Osteoarthritic Culture Model. J Orthop Res 2005;23:118–126. [PubMed: 15607883]
8. Ramage L, Nuki G, Salter DM. Signalling Cascades in Mechanotransduction: Cell–Matrix Interactions and Mechanical Loading. Scand J Med Sci Sports 2009;19:457–469. [PubMed: 19538538]
9. Kiviranta I, Jurvelin J, Tammi M, Säämänen AM, Helminen HJ. Weight Bearing Controls Glycosaminoglycan Concentration and Articular Cartilage Thickness in the Knee Joints of Young Beagle Dogs. Arthritis Rheum 1987;30:801–809. [PubMed: 3619962]
10. Helminen, HJ.; Kiviranta, I.; Säämänen, AM.; Jurvelin, JS.; Arokoski, J.; Oettmeier, R.; Abendroth, K.; Roth, AJ.; Tammi, MI. Articular Cartilage and Osteoarthritis. Kuettner, KE.; Hascall, VC.; Schleyerbach, R., editors. Raven; New York: 1992. p. 501-510.
11. Flannery CR, Hughes CE, Schumacher BL, Tudor D, Aydelotte MB, Kuettner KE, Caterson B. Articular Cartilage Superficial Zone Protein (SZP) is Homologous to Megakaryocyte Stimulating Factor Precursor and Is a Multifunctional Proteoglycan With Potential Growth-Promoting, Cytoprotective, and Lubricating Properties in Cartilage Metabolism. Biochem Biophys Res Commun 1999;254:535–541. [PubMed: 9920774]
12. Roughley PJ. The Structure and Function of Cartilage Proteoglycans. Eur Cells Mater 2006;12:92–101.
13. Woo SL, Akeson WH, Jemmott GF. Measurements of Nonhomogeneous, Directional Mechanical Properties of Articular Cartilage in Tension. J Biomech 1976;9:785–791. [PubMed: 1022791]
14. Roth V, Mow VC. The Intrinsic Tensile Behavior of the Matrix of Bovine Articular Cartilage and Its Variation With Age. J Bone Jt Surg Am Vol 1980;62:1102–1117.
15. Ateshian, GA.; Mow, VC. Basic Orthopaedic Biomechanics and Mechano-Biology. Mow, VC.; Huiskes, R., editors. Lippincott Williams & Wilkins; Philadelphia: 2005. p. 447-494.
16. Quinn TM, Grodzinsky AJ, Hunziker EB, Sandy JD. Effects of Injurious Compression on Matrix Turnover Around Individual Cells in Calf Articular Cartilage Expants. J Orthop Res 1998;16:490–499. [PubMed: 9747792]
17. Loening AM, James IE, Levenston ME, Badger AM, Frank EH, Kurz B, Nuttall ME, Hung HH, Blake SM, Grodzinsky AJ, Lark MW. Injurious Mechanical Compression of Bovine Articular

Cartilage Induces Chondrocyte Apoptosis. Arch Biochem Biophys 2000;381:205–212. [PubMed: 11032407]

18. Setton LA, Mow VC, Muller FJ, Pita JC, Howell DS. Mechanical Properties of Canine Articular Cartilage Are Significantly Altered Following Transaction of the Anterior Cruciate Ligament. J Orthop Res 1994;12:451–463. [PubMed: 8064477]
19. Jeffrey JE, Gregory DW, Aspden RM. Matrix Damage and Chondrocyte Viability Following a Single Impact Load on Articular Cartilage. Arch Biochem Biophys 1995;322:87–96. [PubMed: 7574698]
20. Kurz B, Jin M, Patwari P, Cheng DM, Lark MW, Grodzinsky AJ. Biosynthetic Response and Mechanical Properties of Articular Cartilage After Injurious Compression. J Orthop Res 2001;19:1140–1146. [PubMed: 11781016]
21. Patwari P, Cook MN, DiMicco MA, Blake SM, James IE, Kumar S, Cole AA, Lark MW, Gordzinsky AJ. Proteoglycan Degradation After Injurious Compression of Bovine and Human Articular Cartilage In Vitro: Interaction With Exogeneous Cytokines. Arthritis Rheum 2003;48:1292–1301. [PubMed: 12746902]
22. Buschmann MD, Gluzband YA, Grodzinsky AJ, Hunziker EB. Mechanical Compression Modulates Matrix Biosynthesis in Chondrocyte/Agarose Culture. J Cell Sci 1995;108:1497–1508. [PubMed: 7615670]
23. Lee DA, Bader DL. Compressive Strains at Physiological Frequencies Influence the Metabolism of Chondrocytes Seeded in Agarose. J Orthop Res 1997;15:181–188. [PubMed: 9167619]
24. Lee JH, Fitzgerald JB, DiMicco MA, Grodzinsky AJ. Mechanical Injury of Cartilage Explants Causes Specific Time-Dependent Changes in Chondrocyte Gene Expression. Arthritis Rheum 2005;52:2386–2395. [PubMed: 16052587]
25. Kisiday JD, Jin M, DiMicco MA, Kurz B, Grodzinsky AJ. Effects of Dynamic Compressive Loading on Chondrocyte Biosynthesis in Self-Assembling Peptide Scaffolds. J Biomech 2004;37:595–604. [PubMed: 15046988]
26. Chowdhury TT, Bader DL, Shelton JC, Lee DA. Temporal Regulation of Chondrocyte Metabolism in Agarose Constructs Subjected to Dynamic Compression. Arch Biochem Biophys 2003;417:105–111. [PubMed: 12921786]
27. Chowdhury TT, Bader DL, Lee DA. Anti-Inflammatory Effects of IL-4 and Dynamic Compression in IL-1β Simulated Chondrocytes. Biochem Biophys Res Commun 2006;339:241–247. [PubMed: 16297873]
28. Ragan PM, Chin VI, Hung HH, Masuda K, Thonar EJ, Arner EC, Grodzinsky AJ, Sandy JD. Chondrocyte Extracellular Matrix Synthesis and Turnover Are Influenced by Static Compression in a New Alginate Disk Culture System. Arch Biochem Biophys 2000;383:256–264. [PubMed: 11185561]
29. Saha AK, Mazumdar JN, Kohles SS. Prediction of Growth Factor Effects on Engineered Cartilage Composition Using Deterministic and Stochastic Modeling. Ann Biomed Eng 2004;32:871–879. [PubMed: 15255217]
30. Saha AK, Mazumdar JN, Kohles SS. Dynamic Matrix Composition in Engineered Cartilage With Stochastic Supplementation of Growth Factors. Australas Phys Eng Sci Med 2005;28:97–104. [PubMed: 16060315]
31. Saha AK, Kohles SS. Cell-Matrix Modeling of Anabolic and Catabolic Dynamics on Cartilage Biomolecule Regulation. Comput Math Methods Med. 2010 in press.
32. Kohles SS, Nève N, Zimmerman JD, Tretheway DC. Stress Analysis of Microfluidic Environments Designed for Isolated Biological Cell Investigations. ASME J Biomech Eng 2009;131(12):121006.
33. Wilson ZD, Kohles SS. Two-Dimensional Modeling of Nanomechanical Strains in Healthy and Diseased Single-Cells During Microfluidic Stress Applications. J Nanotech Eng Med 2010;1(2): 021005.
34. Li J, Fu X, Sun X, Sun T, Sheng Z. The Interaction Between Epidermal Growth Factor and Matrix Metalloproteinases Induces the Development of Sweat Glands in Human Fetal Skin. J Surg Res 2002;106(2):258–263. [PubMed: 12175976]

35. Kim W, Tretheway DC, Kohles SS. An Inverse Method for Predicting Tissue-Level Mechanics From Cellular Mechanical Input. J Biomech 2009;42(3):395–399. [PubMed: 19135204]
36. Wilson CG, Bonassar LJ, Kohles SS. Modeling the Dynamic Composition of Engineered Cartilage. Arch Biochem Biophys 2002;408:246–254. [PubMed: 12464278]
37. Freed LE, Hollander AP, Martin I, Barry JR, Langer R, Vunjak-Novakovic G. Chondrogenesis in a Cell-Polymer-Bioreactor System. Exp Cell Res 1998;240:58–65. [PubMed: 9570921]
38. Vunjak-Novakovic G, Obradovic B, Martin I, Bursac PM, Langer R, Freed LE. Dynamic Cell Seeding of Polymer Scaffolds for Cartilage Tissue Engineering. Biotechnol Prog 1998;14:193–202. [PubMed: 9548769]
39. Urban JP. The Chondrocyte: A Cell Under Pressure. Br J Rheumatol 1994;33:901–908. [PubMed: 7921748]
40. Martinac B. Mechanosensitive Ion Channels: Molecules of Mechanotransduction. J Cell Sci 2004;117:2449–2460. [PubMed: 15159450]
41. Ingber D. Integrins as Mechanochemical Transducers. Curr Opin Cell Biol 1991;3:841–848. [PubMed: 1931084]
42. Wright M, Jobanputra P, Bavington C, Salter DM, Nuki G. Effects of Intermittent Pressure-Induced Strain on the Electrophysiology of Cultured Human Chondrocytes: Evidence for the Presence of Stretch-Activated Membrane Ion Channels. Clin Sci 1996;90:61–71. [PubMed: 8697707]
43. Kim YJ, Grodzinsky AJ, Plaas AHK. Compression of Cartilage Results in Differential Effects on Biosynthetic Pathways for Aggrecan Link Protein, and Hyaluronan. Arch Biochem Biophys 1996;328:331–340. [PubMed: 8645012]
44. Lee HS, Millward-Sadler SJ, Wright MO, Nuki G, Salter DM. Integrin and Mechanosensitive Ion Channel-Dependent Tyrosine Phosphorylation of Focal Adhesion Proteins and β-Catenin in Human Articular Chondrocytes After Mechanical Stimulation. J Bone Miner Res 2000;15:1501–1509. [PubMed: 10934648]
45. Millward-Sadler SJ, Wright MO, Davies LW, Nuki G, Salter DM. Mechanotransduction Via Integrins and Interleukin-4 Results in Altered Aggrecan and Matrix Metalloproteinase 3 Gene Expression in Normal, But Not Osteoarthritic, Human Articular Chondrocytes. Arthritis Rheum 2000;43:2091–2099. [PubMed: 11014361]
46. Wu QQ, Chen Q. Mechanoregulation of Chondrocyte Proliferation, Maturation, and Hypertrophy: Ion-Channel Dependent Transduction of Matrix Deformation Signals. Exp Cell Res 2000;256:383–391. [PubMed: 10772811]
47. Fanning PJ, Emkey G, Smith RJ, Grodzinsky AJ, Szasz N, Trippel SB. Mechanical Regulation of Mitogen-Activated Protein Kinase Signaling in Articular Cartilage. J Biol Chem 2003;278:50940–50948. [PubMed: 12952976]
48. Murata M, Bonassar LJ, Wright M, Mankin HJ, Towle CA. A Role for the Interleukin-1 Receptor in the Pathway Linking Static Mechanical Compression to Decreased Proteoglycan Synthesis in Surface Articular Cartilage. Arch Biochem Biophys 2003;413:229–235. [PubMed: 12729621]
49. Szafranski JD, Grodzinsky AJ, Burger E, Gaschen V, Hung HH, Hunziker EB. Chondrocyte Mechanotransduction: Effects of Compression on Deformation of Intracellular Organelles and Relevance to Cellular Biosynthesis. Osteoarthritis Cartilage 2004;12:937–946. [PubMed: 15564060]
50. Fitzgerald JB, Jin M, Dean D, Wood DJ, Zheng MH, Grodzinsky AJ. Mechanical Compression of Cartilage Explants Induces Multiple Time Dependent Gene Expression Patterns and Involves Intracellular Calcium and Cyclic AMP. J Biol Chem 2004;279:19502–19511. [PubMed: 14960571]
51. Vincent TL, Hermansson MA, Hansen UN, Amis AA, Saklatvala J. Basic Fibroblast Growth Factor Mediates Transduction of Mechanical Signals When Articular Cartilage Is Loaded. Arthritis Rheum 2004;50:526–533. [PubMed: 14872495]
52. Perkins GL, Derfoul A, Ast A, Hall DJ. An Inhibitor of the Stretch-Activated Cation Receptor Exerts a Potent Effect on Chondrocyte Phenotype. Differentiation 2005;73:199–211. [PubMed: 16026542]

53. Fitzgerald JB, Jim M, Grodzinsky AJ. Shear and Compression Differentially Regulate Clusters of Functionally Related Temporal Transcription Patterns in Cartilage Tissue. J Biol Chem 2006;281:24095–24103. [PubMed: 16782710]

54. Mouw JK, Imler SM, Levenston ME. Ion-Channel Regulation of Chondrocyte Matrix Synthesis in 3D Culture Under Static and Dynamic Compression. Biomech Model Mechanobiol 2007;6:33–41. [PubMed: 16767453]

55. Fitzgerald JB, Jin M, Chai DH, Siparsky P, Fanning P, Grodzinsky AJ. Shear- and Compression-Induced Chondrocyte Transcription Requires MAPK Activation in Cartilage Explants. J Biol Chem 2007;283(11):6735–6743. [PubMed: 18086670]

56. Niehoff A, Offermann M, Dargel J, Schmidt A, Brüggemann GP, Bloch W. Dynamic and Static Mechanical Compression Affects Akt Phosphorylation in Porcine Patellofemoral Joint Cartilage. J Orthop Res 2008;26:616–623. [PubMed: 18050339]

57. Vincent TL, McLean CJ, Full LE, Peston D, Saklatvala J. FGF-2 Is Bound to Perlecan in the Pericellular Matrix of Articular Cartilage, Where It Acts as a Chondrocyte Mechanotransducer. Osteoarthritis Cartilage 2007;15:752–763. [PubMed: 17368052]

58. Grodzinsky AJ, Levenston ME, Jin M, Frank EH. Cartilage Tissue Remodeling in Response to Mechanical Forces. Annu Rev Biomed Eng 2000;2:691–713. [PubMed: 11701528]

59. Sah RL, Kim YJ, Doong JH, Grodzinsky AJ, Plaas AHK, Sandy JD. Biosynthetic Response of Cartilage Explants to Dynamic Compression. J Orthop Res 1989;7:619–636. [PubMed: 2760736]

60. Guilak F, Meyer FC, Ratcliffe A, Mow VC. The Effects of Matrix Compression on Proteoglycan Metabolism in Articular Cartilage Explants. Osteoarthritis Cartilage 1994;2:91–101. [PubMed: 11548233]

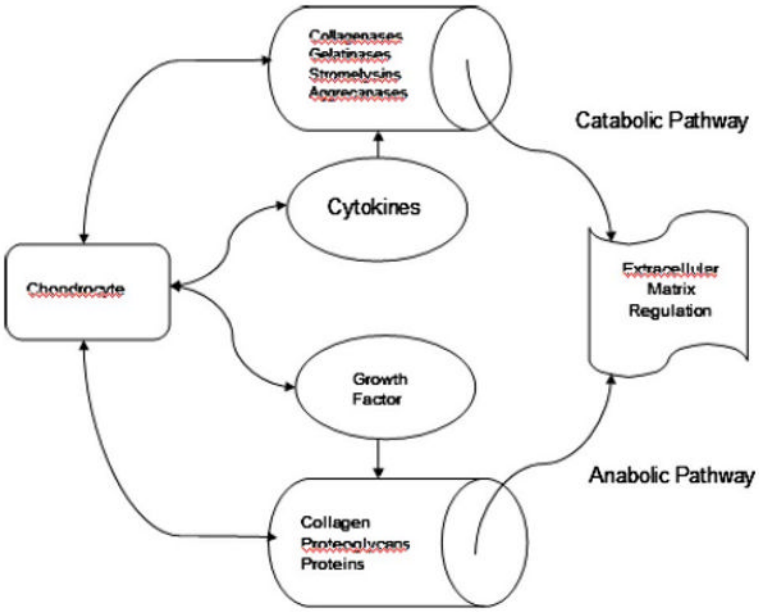

Fig. 1. Schematic diagram of the simplified interactions between the critical influences on extracellular matrix turnover associated with anabolic and catabolic pathways

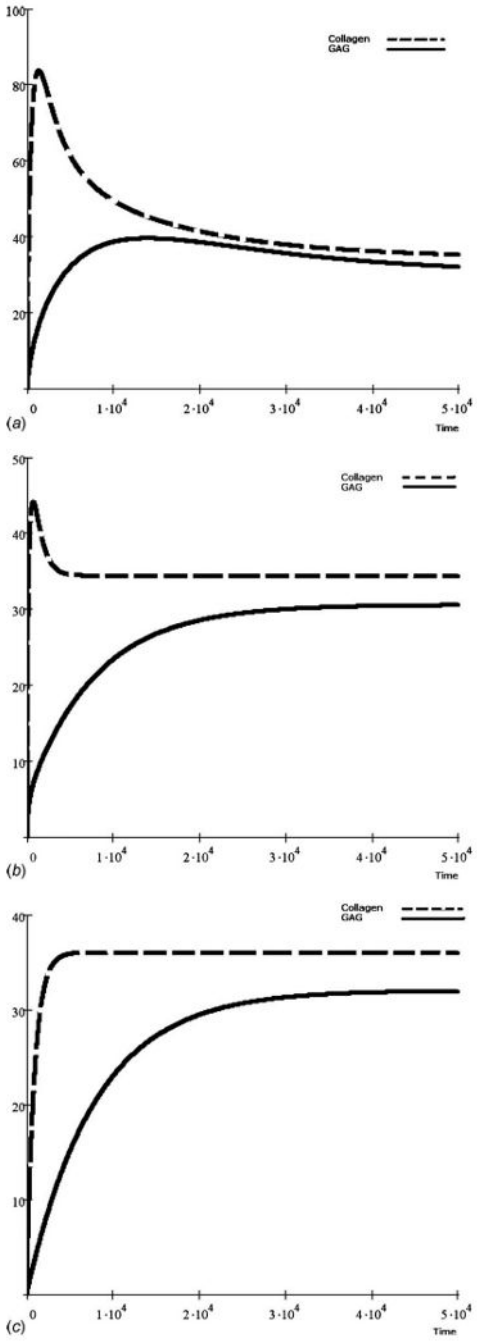

Fig. 2.

Simulated time-dependent GAG and collagen accumulation from experimental parameters where collagen content was greater than GAG content, each with unique kinetic characteristics [36]. Abundance is shown over dimensionless time with mechanical stimuli having a consistent scaling factor of $\rho_1(T)=\rho_2(T) = 1$ and load components of (*a*) $\xi_1(T) = \xi_2(T)=0.0$, (*b*) $\xi_1(T)=\xi_2(T)=0.02$, and (*c*) $\xi_1(T) = \xi_2(T) = 1.0$.

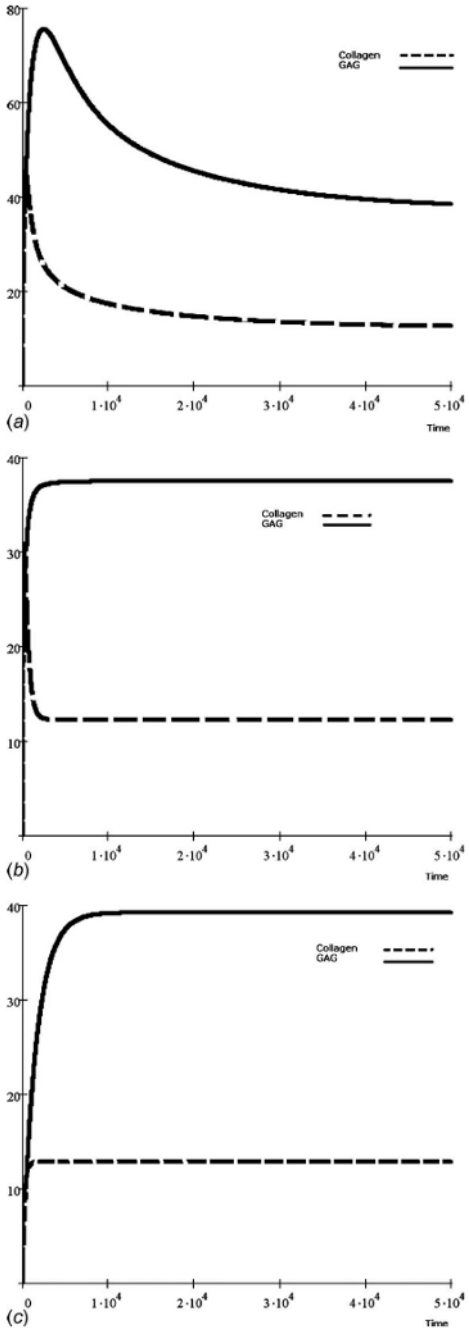

Fig. 3.

GAG and collagen accumulation over time from an experimental scenario with GAG content much greater than collagen content, albeit with differing dynamic characteristics [37]. The mechanical loads were included with a consistent scaling factor of $\rho_1(T)=\rho_2(T) = 1$ and load components of (*a*) $\xi_1(T) = \xi_2(T) = 0.0$, (*b*) $\xi_1(T) = \xi_2(T) = 0.02$, and (*c*) $\xi_1(T) = \xi_2(T) = 1.0$.

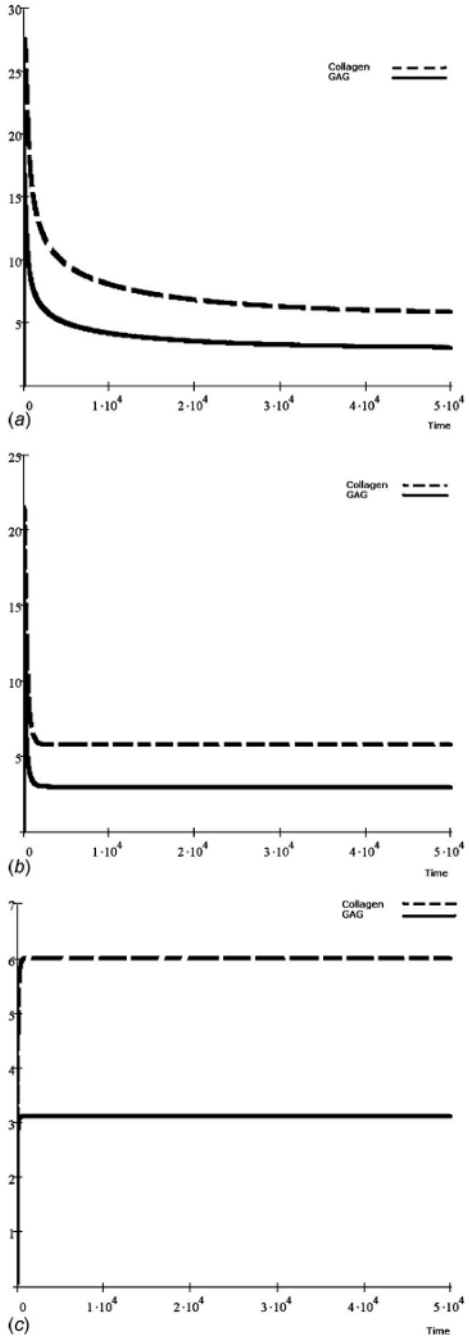

Fig. 4.

Dynamic GAG and collagen accumulation modeled from experiments with collagen content being both greater in content and similar in form as the GAG accumulation [38]. As with all of the models, mechanical stimulation had a consistent scaling factor of $\rho_1(T)=\rho_2(T) = 1$ and load components of (*a*) $\xi_1(T) = \xi_2(T) = 0.0$, (*b*) $\xi_1(T) =\xi_2(T) = 0.02$, and (*c*) $\xi_1(T) = \xi_2(T) = 1.0$.

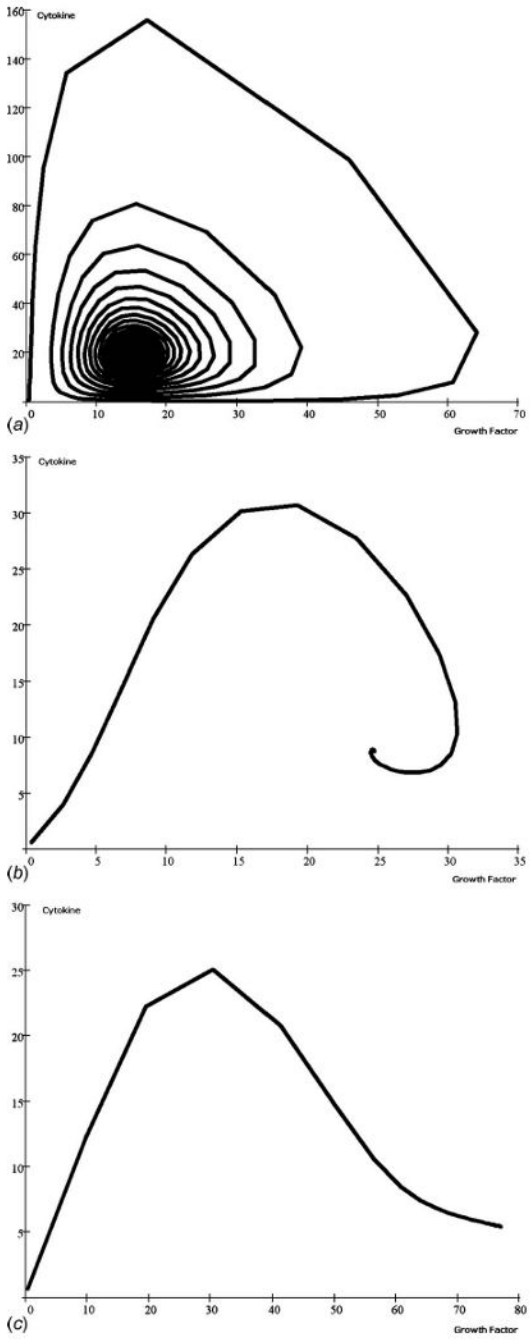

Fig. 5.

The cyclic phase-limit solutions describing the steady state progression in the relationship between growth factor and cytokine accumulation. In this analysis, time dependence was not included, thus eliminating the biokinetic rate differences between the three experimental input studies [36–38]. These scenarios were all run with constant scaling factors of $\rho_1(T)=\rho_2(T)=1$. Mechanical load components were constrained to (*a*) $\xi_1(T)=\xi_2(T)=1.0$, (*b*) $\xi_1(T)=\xi_2(T)=25.0$, and (*c*) $\xi_1(T) = \xi_2(T) = 100.0$. As development progresses during dimensionless culture time, the relative relationship loops clockwise as well as from the outward toward the central steady state condition until the mechanical stimulus disrupts the

spiral progression, leading to an increase in growth factors with low cytokine levels, and presumably active ECM synthesis.

Table 1

Metabolic interplay parameters developed from a systems biology approach for describing nanoscale molecular homeostasis [31]

Parameter	Description	Relationship or value
α_1	Synthesis rate of cytokines	$\alpha_1=0.048+\beta_1$
α_2	Growth rate of growth factor (GF)	$\alpha_2=0.044+\beta_2$
β_1	Decay rate of cytokines	$\beta_1=\frac{1}{\tau_1}\left\{\frac{\Omega_2-G_{ss}}{G_{ss}+1-\Omega_2}\right\}$
β_2	Natural decay rate of GF	$\beta_2=\frac{1}{\tau_2}\left\{\frac{C_{ss}-\Omega_1}{\Omega_1-C_{ss}-1}\right\}$
Ω_1	Pivotal parameter for GF	$C_{ss}-1<\Omega_1<C_{ss}$
Ω_2	Pivotal parameter for cytokines	$G_{ss}<\Omega_2<G_{ss}+1$

Table 2

Biokinetic rates derived previously from three independent cartilage engineering experiments each having unique biochemical modulation results [29,30]

							Rates: growth (λ) and decay (δ)	
							λ_{GAG}	$\lambda_{collagen}$
Scaffold	**Cell type**	**Ref.**	**GAG_{ss}**	**τ_{GAG} (days)**	**$Collagen_{ss}$**	**$\tau_{collagen}$ (days)**	δ_{GAG}	$\delta_{collagen}$
PGA	BAC	37	6.8% ww	31.3	3.7% ww	15.9	3.256×10^{-2}	6.672×10^{-2}
							6.139×10^{-4}	3.837×10^{-3}
PGA	BAC	36	6.1% dw	187.0	6.5% dw	18.9	5.474×10^{-3}	5.400×10^{-2}
							1.264×10^{-4}	1.108×10^{-3}
PGA	BAC	38	1.6% ww	22.2	2.4% ww	16.7	5.900×10^{-2}	6.800×10^{-2}
							1.400×10^{-2}	8.363×10^{-3}

PGA=polyglycolic acid.

BAC=bovine articular cartilage.

ww, dw=wet weight, dry weight.